Intermetallics 103 (2018) 78–87

Contents lists available at ScienceDirect

Intermetallics

journal homepage: www.elsevier.com/locate/intermet

Notch fracture toughness of body-centered-cubic (TiZrNbTa)–Mo high-entropy alloys

Shao-Ping Wang[a,b], Evan Ma[c], Jian Xu[a,*]

[a] Shenyang National Laboratory for Materials Science, Institute of Metal Research, Chinese Academy of Sciences, 72 Wenhua Road, Shenyang, 110016, China
[b] University of Chinese Academy of Sciences, 19(A) Yuquan Road, Beijing, 100049, China
[c] Department of Materials Science and Engineering, The Johns Hopkins University, Baltimore, MD, 21218, USA

ARTICLE INFO

Keywords:
High-entropy alloys
Fracture toughness
BCC structure
Nanoindentation
Dislocation

ABSTRACT

The notch fracture toughness (K_Q) and its dependence on Mo concentration in as-cast body-centered-cubic $(TiZrNbTa)_{100-x}Mo_x$ high-entropy alloys have been measured at room temperature. It is shown that the increase of Mo concentration results in a significant reduction in fracture toughness, with the K_Q decreasing from 28.5 MPa√m for the Mo-free TiZrNbTa quaternary alloy to 18.7 MPa√m for the TiZrNbTaMo quinary alloy. The K_Q of these HEAs scales inversely with increasing ($d + s$) electrons per atom. The fracture mode under Mode I loading transists from monolithic intergranular fracture for Mo-free TiZrNbTa to completely transgranular cleavage for the TiZrNbTaMo alloy. The brittleness is consistent with the known effects of refractory solutes on increasing the brittle-to-ductile transition temperature in Nb-based solutions. The embrittlement effect with alloying (especially Mo) is also attributable to the elevation of the critical temperature (T_0), making the activation to overcome lattice resistance to dislocation motion increasingly difficult. The low ratio T/T_0 (T = 300 K in our case) can in fact be inferred from the very small activation volume ($3b^3$) measured for TiZrNbTa and TiZrNbTaMo.

1. Introduction

With multiple principal elements, high-entropy alloys (HEAs) open up a vast compositional space to explore new materials for useful properties [1–5]. In this new family of complex concentrated alloys (CCAs), refractory HEAs based on early transition metals, such as Ti, Zr, Hf, V, Nb, Ta, Mo and W [6–10], are of considerable interest. These alloys are single-phase body-centered cubic (bcc) solid solutions, having a high yield strength at a level of σ_y = 900–1600 MPa and appreciable compressive plasticity. In addition, several refractory HEAs show tensile strain to failure of 4–30% [11–13]. However, little is known about the fracture toughness of these new alloys [14–16].

Due to the excellent biocompatibility of refractory elements [17–19], it was proposed to develop new HEAs applicable for biomedical implants, in the Ti–Zr–Nb–Ta–Mo system with a composition starting from the equiatomic TiZrNbTaMo [20–23]. Such efforts are motivated by searching for the alloys with high strength, tolerable toughness and good wear resistance superior to titanium alloys (e.g., Ti6Al4V), in order to be used as bearing surfaces. In our previous work [21], it has been shown that the mechanical properties of the arc-melted $(TiZrNbTa)_{100-x}Mo_x$ ($0 \le x \le 20$) HEAs with bcc structure are dependent on Mo concentration. The Young's modulus (E), microhardness (H_v) and compressive yield stress (σ_y) of these alloys all increase linearly with the Mo concentration. The σ_y increases from 1020 MPa at the quaternary TiZrNbTa up to 1460 MPa at the quinary TiZrNbTaMo. However, this is accompanied by a reduction in the apparent plastic strain, from > 25% down to < 6%. For these alloys to be useful in applications, it is important to investigate their fracture behavior under Model I loading, including the composition dependence of their fracture toughness. Meanwhile, notch fracture toughness as an apparent property has been widely used to preliminarily assess the material toughness [24,25], particularly for material screening in toughness optimization, even though introducing a somewhat overestimation in fracture toughness due to the blunting effect of notch root without fatigue pre-cracking on the samples.

It is well known that the fracture toughness and the brittle-to-ductile transition (BDT) depend strongly on the dislocation activities (including the nucleation, mobility and multiplication of dislocations) at the crack tips, in particular for bcc metals [26–29]. The dislocation behavior is currently poorly understood for bcc refractory HEAs. It has been suggested that like normal bcc metals, their plastic deformation is generally controlled by screw dislocations, and the kink-pair nucleation

* Corresponding author.
E-mail address: jianxu@imr.ac.cn (J. Xu).

https://doi.org/10.1016/j.intermet.2018.10.008
Received 8 August 2018; Received in revised form 8 October 2018; Accepted 8 October 2018

mechanism and local variations in the dislocation core structure play an important role [30–32]. Some of the bcc HEAs are likely to be brittle at room temperature, similar to some refractory bcc metals.

Recently, nanoindentation testing has been used to characterize the deformation and dislocation behavior of HEAs [33–37]. By characterizing the indentation pop-in of fcc FeCoCrNiMn HEA (Cantor alloy) [33], it is shown that a vacancy-medicated heterogeneous dislocation nucleation may be the mechanism for the onset of plasticity. It was suggested that vacancy migration in this HEA involves the cooperative motion of several atoms. Using the nanoindentation strain-rate jump testing, the activation volume and strain rate sensitivity (SRS) of the deformation process have been determined for the Cantor alloy [36], suggesting a high lattice friction that has to be overcome by thermal activation in this typical HEA. There have also been several studies on the activation volume and SRS in bcc HEAs [31,32,38]. However, the understanding of activation parameters in HEAs is generally in its rudimentary stage.

The purpose of this paper is threefold. First, we report the notch fracture toughness (K_Q) measurements and the dependence of K_Q on Mo concentration in the arc-melted $(TiZrNbTa)_{100\text{-}x}Mo_x$ high-entropy alloys with bcc structure at room temperature. The results highlight the Mo alloying effect on the toughness of these HEAs. Meanwhile, the crack initiation and propagation under Model I loading are examined. Second, two HEAs, TiZrNbTa and TiZrNbTaMo, are selected as the representative to determine the apparent activation volumes of dislocation mobility and SRS with nanoindentation testing. Finally, the toughness and fracture mechanism, as well as the correlation of fracture toughness with dislocation behavior in these HEAs are discussed.

2. Experimental

Elemental bulk materials with purity higher than 99.9% (in weight percentage) were used as starting materials for alloy ingot fabrication. A series of alloys with nominal composition of $(TiZrNbTa)_{100\text{-}x}Mo_x$ ($x = 0$, 5, 10, 15, 20 in atomic percentage) were processed using arc melting. The latter was carried out under a Ti-gettered argon atmosphere in a water-cooled copper hearth, subjected to re-melting and flipping of several repetitions to ensure compositional homogeneity.

For the notch fracture toughness measurements, rectangular samples with a dimension of $B = 4$ mm, $W = 8$ mm and $S = 32$ mm were taken from the center portion of the as-cast ingots, suing electro-discharge machining and polishing. With the single-edge notched bending (SENB) specimens, a straight through notch with a root radius of approximately 150 μm and a length of 0.45–0.55 W was processed using a diamond wire saw. Three-point bending (3 PB) tests of the notched samples were carried out on a 10 kN Shimadzu AG-X testing machine (Shimadzu, Japan) at a constant displacement rate of 0.05 mm/min at room temperature. The cross-head displacement was used for recording the load-displacement curves. To confirm the data reproducibility, at least four samples were tested for each alloy.

To observe the crack propagation path, the outmost side-surfaces near the notch root of the representative specimens after cracking under open-stressing loading were characterized using electronic back-scattered diffraction (EBSD) imaging attached on Supra 55 scanning electron microscope (SEM) (Zeiss, Germany). Fractured surfaces of the samples subjected to 3 PB overloading were examined in a Quanta 600 SEM (FEI, Eindhoven, Netherlands).

The equi-atomic quaternary ($x = 0$) and quinary ($x = 20$) alloys were selected as the representative for nanoindentation measurements. The machined cuboidal sample surfaces of both alloys were mechanically ground with SiC abrasive paper to 2000 grits, and then polished with 1-μm Al_2O_3 suspension followed by 0.04-μm colloidal silica. The as-polished surfaces were subsequently ion-milled to remove the residual-stress layer and possible surface damage, followed by ultrasonic cleaning in ethanol and distilled water. The ultimate average surface roughness (R_a) was determined to be less than 3 nm using a LEXT OLS4000 laser scanning confocal microscope (Olympus, USA).

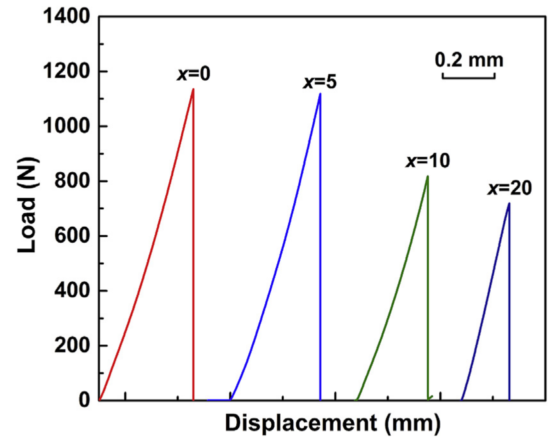

Fig. 1. Load versus load-point displacement curves of typical notched samples under 3 PB loading for as-cast $(TiZrNbTa)_{100\text{-}x}Mo_x$ ($0 \le x \le 20$) HEAs.

Nanoindentation measurements were carried out at room temperature using a Nano Indenter G200 (Agilent Technologies, USA) using a Berkovich indenter with a tip radius of 20 nm. Indentation was performed in depth-control mode with a depth limit of 400 nm, dwell time of 10 s at peak loading, and data acquisition frequency of 5 Hz. Note that the nanoindentation hardness was confirmed to be independent of the selected indentation depth. Three strain rates ($\dot{P}/P$) of 0.001, 0.005 and 0.05 s^{-1} were used, which is equivalent to indentation strain rates ($\dot{h}/h$) of 0.0005, 0.0025 and 0.025 s^{-1} ($\dot{h}/h = \frac{1}{2}\dot{P}/P$). At least 10 indentations on several randomly-selected grains were performed for each applied strain rate.

3. Results

3.1. Dependence of fracture toughness on Mo concentration

Fig. 1 shows typical load-displacement curves of SENB samples during loading for the arc-melted $(TiZrNbTa)_{100\text{-}x}Mo_x$ alloy series. It is notable that all samples failed under limited elastic strain without visible plasticity during cracking and ultimate fracture. This finding indicates that the energy consumption caused by crack initiation ahead of the notch root is the major contributor to the toughness. Once the crack initiates at the stress-concentrated site of the notch, it rapidly develops into unstable fracture. According to ASTM standard E399 [39], the notch toughness (K_Q) of these alloys is determined using the following equations,

$$K_Q = \frac{PS}{BW^{3/2}} \cdot f\left(\frac{a}{W}\right) \tag{1}$$

$$f\left(\frac{a}{W}\right) = 3\sqrt{\frac{a}{W}} \cdot \frac{1.99 - (\frac{a}{W})\left(1 - \frac{a}{W}\right)\left(2.15 - 3.93\frac{a}{W} + 2.7\left(\frac{a}{W}\right)^2\right)}{2\left(1 + 2\frac{a}{W}\right)\left(1 - \frac{a}{W}\right)^{3/2}} \tag{2}$$

where P is the peak force loaded on the samples, S is the span between the two support rollers, B is the specimen thickness, W is the specimen width, and a is the initial crack size. Table 1 summarizes the K_Q value of each alloy.

Fig. 2 shows a plot of K_Q against Mo concentration in the (TiZrNbTa)−Mo HEAs. It is seen that the K_Q rapidly drops from 28.5 MP√m for the Mo-free alloy down to 22.5 MP√m for the 5 at.% Mo alloy. In other words, addition of 5 at.% Mo in TiZrNbTa HEA significantly deteriorates the alloy toughness. On further increasing Mo concentration to 20 at.%, the K_Q is gradually reduced down to 18.7 MP√m. Apparently, with respect to the TiZrNbTa HEA the